

Article

Analysis of Spatial-temporal behavior pattern of the Share Bike Users during COID-10 Pandemic in Beijing

Xinwei Chai ^{1,2,‡}, Xian Guo ^{1,†,‡,*}, Jihua Xiao ² and Jie Jiang ¹

¹ Beijing University of Civil Engineering and Architecture, 102616 Beijing, China; guoxian@bucea.edu.cn (X.G.); jiangjie@bucea.edu.cn (J.J.)

² China Location-Based Service, 100191 Beijing, China; xw.chai@chinalbs.org (X.C.); jh.xiao@chinalbs.org (J.X.)

* Correspondence: guoxian@bucea.edu.cn; Tel.: +86 (010) 6120 9335

Version May 13, 2020 submitted to ISPRS Int. J. Geo-Inf.

Abstract: During the epidemics of COVID-19, the whole world is experiencing a serious crisis on public health and economy. Detailed information in the behavior of residents during epidemic benefits emergency management when one tries to design intervention strategies and resilience measures. From the perspective of movements, the widely used Bike Sharing System (BSS) in China is capable of characterizing the behavior patterns over time & space within big cities. Although share bikes are playing an important role as data sources in data mining, they could be of help but are rarely reported in pandemic-related researches. Based on the share bike records in Beijing, we constructed a behavior pattern analysis framework, then analyzed the spatiotemporal behavior patterns of residents, figured out the key time nodes of different pandemic periods, and demonstrated the variations in mobility due to the onset of the COVID-19 threat and administrative restrictions. The impact of the pandemic was assessed by performing co-location analysis between share bike usage and POIs (Point Of Interest). Classification of POIs is helpful to distinguish the behavior patterns generated by various the productive and social activities. Discussions with evolving confirmed COVID-19 cases suggest the effectiveness and necessity of the public interventions in the COVID-19 containment during the resilience period. These findings provide critical information on how to respond to the current COVID-19 outbreak and other epidemic events.

Keywords: Bike sharing system; COVID-19; behavior pattern; spatiotemporal analysis; co-location analysis

1. Introduction

COVID-19 is a rapidly spreading infectious disease caused by the novel coronavirus SARS-CoV-2, which has now established a global pandemic¹. According to a situation report of WHO², the worldwide total confirmed cases have reached 2,471,136 including 84,287 that of China as of 22 April 2020. It is well-accepted that COVID-19 pandemic inflicts a huge impact on public health and most of the domains of economy, from the Chinese New Year holiday till today (April 2020).

Under the threat of the pandemic, the activities of residents are inevitably influenced and restricted. Since it is associated with productive and social activities, the behavior of residents is used as one of the evaluation indicators for post-disaster reconstruction [1,2]. Measuring the changes of the behavior

¹ [https://www.who.int/emergencies/diseases/novel-coronavirus-2019/technical-guidance/naming-the-coronavirus-disease-\(covid-2019\)-and-the-virus-that-causes-it](https://www.who.int/emergencies/diseases/novel-coronavirus-2019/technical-guidance/naming-the-coronavirus-disease-(covid-2019)-and-the-virus-that-causes-it)

² <https://www.who.int/docs/default-source/coronavirus/situation-reports/20200422-sitrep-93-covid-19.pdf>

of residents is urgent to enhance emergency management and post-disaster recovery of the current COVID-19 outbreak. Current COVID-19-related epidemiological studies mainly focus on transmission dynamics [3,4] and preventive measures [5,6] based on the timeline of outbreak. However, few studies have been reported to analyze quantitatively the spatiotemporal patterns of public behavior during pandemic situations, which is essential for planning preventive strategies and impact assessments on the economy and society. Ferguson et al. [7] have studied two main strategies in the prevention of infectious diseases: *suppression*, case of China and South Korea, with enormous social and economic costs which may cause secondary disasters on health and well-being in the short and longer-term; *mitigation*, case of Great Britain and the United States, may not able to deal with all those with severe disease and resulting in high mortality. Available studies on human mobility patterns during disasters mainly focus on short-term emergencies (e.g., fires and earthquakes) [8,9]. Research on the dynamics of the behavior of residents on a detailed scale during a long-term pandemic is very limited.

The emergence of geospatial big data has great potential to benefit the applications in disease surveillance and disaster response in the past [10–12]. Horanont et al. [13] made use of mobile phone data collected after the 2011 Great Japan Earthquake and provided useful information on how humans react in disaster scenarios and how the evacuation process can be monitored. After the 2015 Nepal Earthquake, Wilson et al. [14] used call detail records pertaining to phone metadata tracking numbers and times of calls to estimate population distribution and socioeconomic status for risk assessment. With geotagged social media data, Chae et al. [15] conducted comprehensive research in spatiotemporal analysis and created a spatial decision support environment that assists in evacuation planning and disaster management. Wesolowski et al. [16] used spatially explicit mobile phone data and malaria prevalence information from Kenya to identify the dynamics of human carriers that drive parasite importation between regions. In this paper, we focus on the spatiotemporal patterns of public behavior response to the COVID-19 pandemic in Beijing, China. To achieve this goal, VGI (Volunteered Geographical Information) plays an important role, in which online surveys and mobile phone positioning data could be references, but they do not cover all the population especially those who care about their privacy and are not willing to offer their precise position [17].

Wide-spread Bike Sharing System (BSS) in China provides a possibility for analyzing such patterns of residents. The 3rd generation BSS (free-floating BSS) emerges in China in 2015 thanks to the rapid development of GIS-based and IoT-based system. Compared to its predecessors, bikes of the 3rd generation BSS (hereinafter referred to as BSS) are no longer constrained by docking stations (so-called free-floating bikes). They are often spread along the roads, congest around shopping/residential areas (RAs), and cover most of the urban residents. As for the city of Beijing, the number of share bikes reached its peak in 2017 and the governors began removing the excess supply afterward. After two years of rapid development and optimization of BSS, the demand and the supply of share bikes meet a balance in 2019, which could be regarded as a stable data source. BSS records contain time and location information of bike usages from anonymous users, providing a valuable indicator of human presence, thus offering a promising alternative data source for increasing the spatial and temporal detail of the mobility and the activities of residents during the pandemic. According to Daxue Consulting [18], in Beijing, 93% of travels less than 5km are quicker done by bike and public transport than with the car, which suggests share bikes have a potential reflection on the local mobility of residents.

The activities of residents in various regions can be easily captured with BSS data, and be used to address the issues such as traffic planning, urban vitality assessment. Du et al. [19] studied the travel patterns of BSS in Nanjing via limited questionnaires. Xu et al. [20] characterized the share bike temporal flow and spatial distribution in Singapore. Kaggle organized a competition of predicting share bike demands³ based on limited entries. There are also studies of BSS focusing on rebalancing strategies [21–23]. While BSS data analytics has been successfully applied in many sectors, their

³ <https://www.kaggle.com/c/bike-sharing-demand>

application in pandemic response is still at its early stages. Moreover, due to limited emerging understanding of the new virus and its transmission mechanism, revealing its impacts on public behavior remains challenging. As far as we know, there is no study on the impact of social events and/or emergencies based on the 3rd generation BSS.

In this study, we constructed a share bike usage based behavior pattern analysis framework to measure period-wise spatiotemporal behavior patterns of residents in Beijing. As preconditioning, a comparison between the same period of 2019 and 2020 was conducted to remove the effect of the Chinese New Year holiday. Identification of the key time nodes in different pandemic periods was conducted by segmenting the whole time series while keeping the maximal similarity inside the segments. In different pandemic periods, we implemented a co-location analysis between the usage patterns and different types of POIs, which reveals the public reactions and assess the impact of the COVID-19 pandemic. Finally, we analyzed the relevance between the change of behavior patterns and the progress of confirmed cases, and assess the effectiveness of suppression strategies. The main novelty of our proposed work is to depict public responses to the progress of COVID-19 from spatiotemporal perspective by interpreting the behavior patterns of residents extracted from long time-sequenced share bike records. Therefore, the impact of the COVID-19 pandemic and the influence of suppression strategy could be analyzed on a citywide scale, providing references in more detail for policy-making and epidemiology research.

The remainder of this paper is organized as follows. Section 2 & 3 describe the study area and proposed methods. Section 4 reports the spatiotemporal change in behavior patterns regarding the local COVID-9 progress and co-location analysis with POIs. Discussions are presented in Section 5 in comparison with the previous year, and relation with confirmed cases during different pandemic periods. Section 6 concludes with some remarks and Section 7 hints future research lines.

2. Study Areas and Data

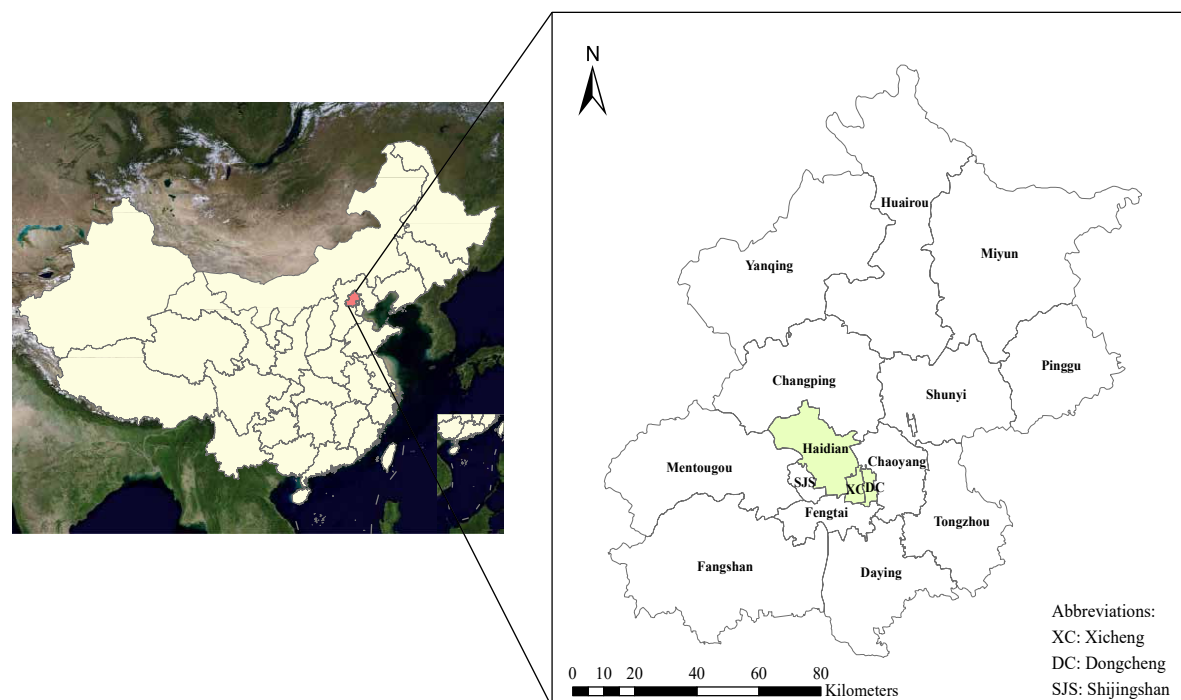


Figure 1. Location map and 16 administrative districts of Beijing.

99 2.1. Study Area

100 This study was conducted in the city of Beijing, the capital of China. As shown in Figure 1,
 101 Beijing locates at the North China Plain, occupying an area of 16,411km² (39.4°-41.6°N, 115.7°-117.4°E).
 102 In 2019, the municipal population of Beijing has reached 21.53 million. According to the Beijing
 103 Health Commission, the COVID-19 confirmed cases⁴ bring the cumulative total in Beijing to 418 by
 104 05 Mar 2020. As a population-importing metropolis, Beijing has taken several efforts in response to
 105 the outbreak. Under this circumstance, the activities of residents have been influenced and showing
 106 special spatiotemporal patterns different from ordinary days.

107 2.2. Description of Data Sets

108 Before describing our results in spatiotemporal patterns of share bike usage, it is first important
 109 to introduce data sets adopted in our experiments.

110 **BSS spatiotemporal data** Temporal positioning datasets come from 900 thousand share bikes
 111 belonging to 4 main BSS operators (Mobike, DiDi Bike, Hellobike, and Ofo) in Beijing. The datasets
 112 date from March 2018 to March 2020 (66.8 GB) and cover 1.5 million uses per day contributed by 11
 113 million users which account for one half of the total population of Beijing. Records of the datasets
 114 contain the positioning and timing information of locking & unlocking of bikes, excluding that of
 115 rebalancing operations. This feature suggests that the movement of bikes is purely done by users. All
 116 analysis we perform is statistically aggregated, removing the ability to characterize the behavior of any
 117 single device. Certain districts (Chaoyang, Fengtai, and Shijingshan) are not comprised in the datasets
 118 due to different policies of local governments.

119 **Points Of Interest (POIs)** POIs of Beijing are collected from AutoNavi API⁵. Each entry is
 120 identified by object_id, recording the address including longitude/latitude information, and
 121 categorized by large_category, mid_category and sub_category. Among hundreds of categories,
 122 we chose six mid ones characterizing productive and social activities: residential area (RA), tech
 123 company, other company, subway station, shopping plaza and supermarket.

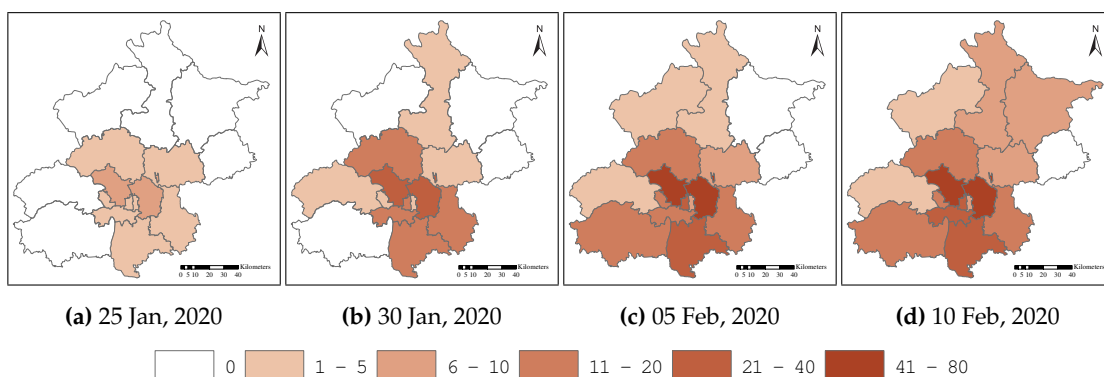


Figure 2. Daily counts of confirmed cases in Beijing.

124 **Locations of Confirmed Cases** The daily cumulative counts of clinically diagnosed cases
 125 subjected to each district from Jan 20 to Mar 5, 2020, were collected from the daily update on the novel
 126 coronavirus pneumonia outbreak dashboard provided by National Health Commission of the People's
 127 Republic of China⁶. According to the timeline [3] of the outbreak, we picked several important dates
 128 shown in Figure 2, visualizing the evolution of the overall pandemic situation of Beijing. To assess the

⁴ http://wjw.beijing.gov.cn/xwzx_20031/wnxw/202003/t20200305_1679143.html (in Chinese)

⁵ <https://lbs.amap.com/api/webservice/guide/api/georegeo> (in Chinese)

⁶ http://www.nhc.gov.cn/xcs/yqtb/list_gzbd.shtml (in Chinese)

¹²⁹ overall behavior pattern changes, we picked out the locations of a total of 87 infected RAs (see Figure
¹³⁰ 3), which were retrieved from Beijing Municipal Health Commission⁷.

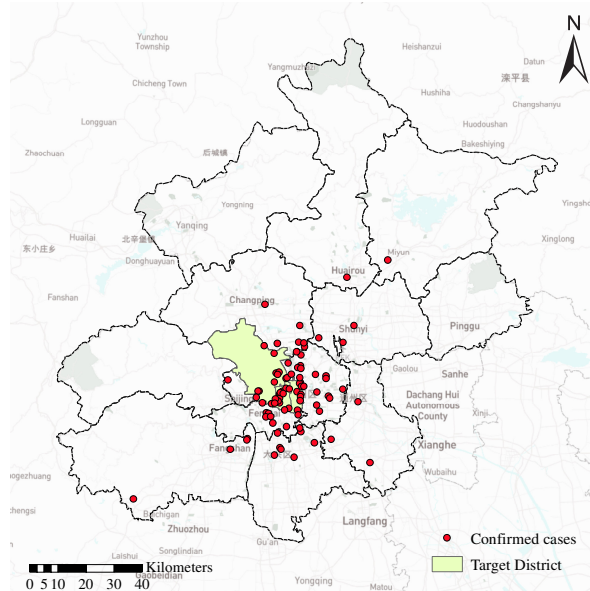


Figure 3. Locations of confirmed cases in Beijing.

¹³¹ 3. Methodology of spatial-temporal behavior pattern analysis

¹³² Figure 4 shows the workflow of our study to assess the reactions of residents to COVID-19 by the
¹³³ above data sets. To deal with large-scale spatial queries of the huge amount of BSS spatiotemporal
¹³⁴ data (66.8GB), we made use of parallel computing all along the two main threads:

- ¹³⁵ 1. GeoSpark [24] acts as an engine processing co-location analysis of POI and BSS data, and the
¹³⁶ result is aggregated and visualized by ArcGIS in the form of heatmaps. This thread is designed
¹³⁷ to quantify the spatial relationships between POIs and share bike usage. Details will be given in
¹³⁸ Section 3.1.
- ¹³⁹ 2. Spark SQL⁸ is used to process temporal queries in BSS data then obtain mean, and standard error.
¹⁴⁰ This thread is to identify key time nodes based on the changes of share bike usage corresponding
¹⁴¹ to COVID-19 and explore the temporal characteristics of share bike usage. Details will be given
¹⁴² in Section 3.2. A next-step process (visualization and optimization) is done in Python.

¹⁴³ Geographic visualization is supported by ESRI ArcGIS 10.7⁹. By synthesizing the results above, we
¹⁴⁴ managed to reveal behavior patterns of share bike usage during the pandemic.

¹⁴⁵ 3.1. Co-location Analysis

¹⁴⁶ To obtain the co-location patterns in such datasets with numerous POIs, we proceeded with
¹⁴⁷ GeoSpark, which allows spatial queries via parallel computing on cluster computing framework Spark.
¹⁴⁸ Among the spatial queries, we utilized `spatial_join(geom1, geom2)`, querying if object `geom1` is
¹⁴⁹ inside `geom2` and `distance_join(geom1, geom2, dist)` querying if the distance of `geom1` and `geom2`
¹⁵⁰ is less than `dist`. These queries are nearly partition independent, recomputing is needed only on the
¹⁵¹ borders of partition, thus our parallel efficiency is high given proper configuration and partitioning.

⁷ http://wjw.beijing.gov.cn/xwzx_20031/wnxw/202003/t20200305_1679143.html (as of March 05, 2020, in Chinese)

⁸ <https://spark.apache.org/>

⁹ <https://www.esri.com/en-us/arcgis/about-arcgis/overview>

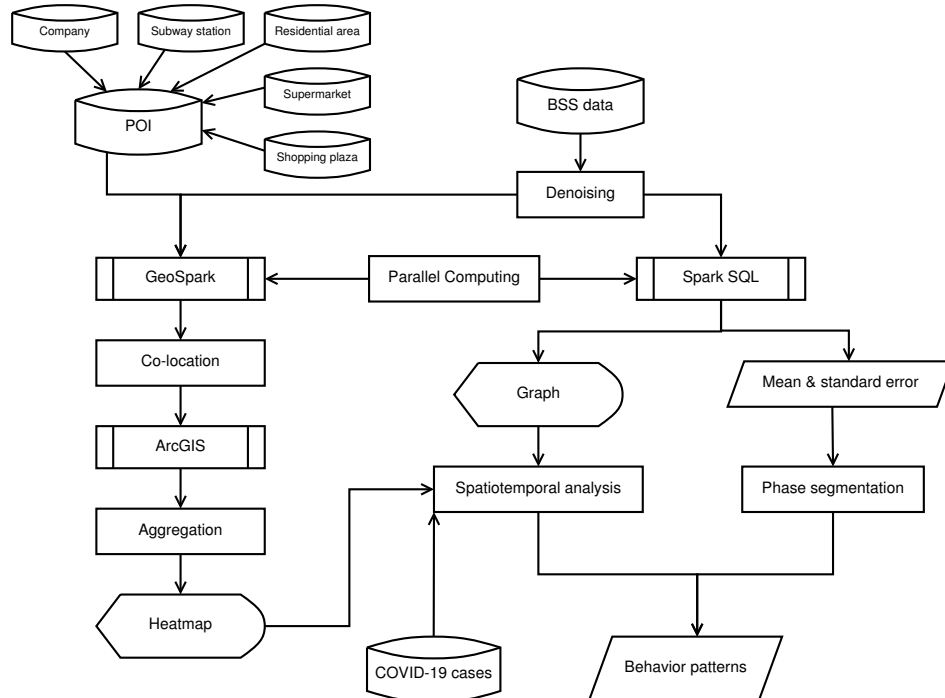


Figure 4. Overview of the proposed behavior pattern mining workflow

152 3.2. Phase Classification

153 In the domain of machine learning, it is often demanded to minimize the predefined loss function
 154 to perform the best classification such that elements within the same cluster are similar and elements
 155 across clusters are different. Likewise, we try to segment the study period into phases that have the
 156 most resembling patterns using k-segmentation.

157 **Definition 1** (k-segmentation). Let $X = \{x_1, x_2, \dots, x_N\}$ be a time series of length N . Given positive integer
 158 $k < N$ and index set $\mathbf{T} = \{n_0, \dots, n_k\}$ with $n_0 = 0$, $n_k = N$ and $\forall i, n_i < n_{i+1}$, a k-segmentation of X is the
 159 set of time series $X_i = \{x_{n_i+1}, \dots, x_{n_{i+1}}\}$ where $0 \leq i \leq k - 1$.

160 To evaluate the quality of k-segmentation, we use $\sigma = \sum_{i=1}^k \sigma_i$ as loss function where σ_i is the
 161 standard deviation of division X_i . The goal is to find the best T to minimize σ , i.e., $\arg \min_{\mathbf{T}} \sigma(\mathbf{T})$.
 162 This problem is solved in time $O(N^2k)$ [25]. In case k and N are small, the optimum can be found via
 163 exhaustive search.

164 4. Experimental results

165 The computation in this paper was done on a computing cluster consisting of 5 machines with
 166 Intel(R) Xeon(R), CPU E5-2640 v2 @2.00GHz, 8 cores, 61.7GB memory, 20480KB cache memory. If we
 167 throw a first glance on the total share bike usage from 01 Jan to 02 Mar, which is 4.56×10^7 in 2019 and
 168 1.61×10^7 in 2020 we found out the total of 2020 is about only one-third of that of 2019 in this period.

169 In this section, we present extensive experimental results of the spatiotemporal change in behavior
 170 patterns regarding the local COVID-9 progress and the association with POIs.

171 4.1. Temporal Patterns of Share Bike Usage

172 To better characterize the behavior patterns with respect to the COVID-19 epidemic dynamics, we
 173 first selected the following important referential dates in Table 1 that could affect the virus transmission
 174 in Beijing:

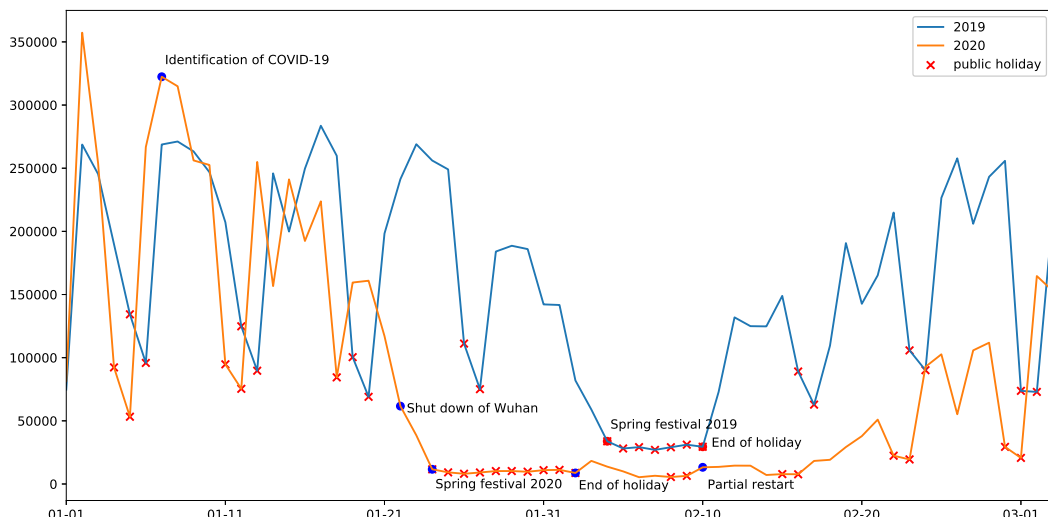
04 Feb 2019	Start of Chinese New Year holiday 2019
10 Feb 2019	End of new year holiday 2019
07 Jan 2020	Identification of COVID-19
22 Jan 2020	Shut down of Wuhan and other 15 cities
24 Jan 2020	Start of Chinese New Year holiday 2020
02 Feb 2020	End of <i>extended</i> New Year holiday 2020
10 Feb 2020	Partial restart of productive and social activities

Table 1. Important dates

175 As the outbreak of COVID-19 coincides with the Chinese New Year holiday 2020, we use the
 176 Chinese New Year holiday of 2019 as a comparison to assess the influence of this period on share bike
 177 usage. It is worth noticing that the Chinese New Year holidays are not equal-length, because that of
 178 2020 is extended by executive order.

179 We compared the share bike usage on rush hours (8:00–09:00) during 64 days from 01 Jan to 02
 180 March 2019 and 01 Jan to 01 March 2020 respectively (data of 29 Feb and 1 March 2020 were brought
 181 backward by one day due to the leap year 2020).

182 Figure 5 illustrates the temporal evolution of share bike usage.

**Figure 5.** Share bike usage during 08:00–09:00 of year 2019 and 2020.

183 The share bike usage drops in mid-January of 2020 and early February of 2019. During these
 184 periods, schools and workplaces were closed as part of the Chinese New Year holiday 2020. The overall
 185 closure was then forced to be extended to mitigate the pandemic.

186 Share bike usage on rush hours exhibits the periodicity of productive activities: high on weekdays
 187 and low on weekends, which fits our general knowledge. However, this pattern does not appear on 10
 188 Feb 2020 when the government declared the partial restart of certain productive and social activities.
 189 This anomaly suggests that the activities were not resumed at all at least until Feb 17, one week after
 190 the partial restart, corresponding to the fact that the impact of the pandemic was lasting till the end of
 191 our study period.

192 Table 2 gives a rough quantitative view over the impact of the pandemic.

193 **Note:** In this paper, we consider share bike usage follows normal distribution, of which 95%
 194 confidence interval is $[\bar{x} - 2\sigma, \bar{x} + 2\sigma]$. Share bike usage data are presented in the form $\bar{x} \pm 2\sigma$.

195 The upper part shows in the rush hours of ordinary days, share bike usage in 2020 is on the same
 196 level as that of 2019, suggesting share bike demand is evolving smoothly. However, the lower part
 197 shows the case of the Chinese New Year holiday, the overall share bike usage drops to less than 40%

Phase	Daily average share bike usage (10^5)		
	08:00-09:00 (on weekdays)	18:00-19:00 (on weekdays)	All-day
02 Jan-20 Jan 2019	2.46 ± 0.59	1.30 ± 0.39	15.0 ± 4.5
02 Jan-20 Jan 2020	2.58 ± 1.10	1.37 ± 0.74	12.7 ± 6.3
	08:00-09:00 (all week)	18:00-19:00 (all week)	All-day
04 Feb-10 Feb 2019	0.30 ± 0.05	0.24 ± 0.08	4.90 ± 1.56
24 Jan-02 Feb 2020	0.10 ± 0.02	0.12 ± 0.03	1.72 ± 0.35

Table 2. Overall comparison of year 2019 and 2020.

198 compared with the same period in 2019, suggesting companies stopped working due to the Chinese
 199 New Year holiday like the case of 2019, and social activities also halted.

200 4.2. Co-location Analysis with POIs

201 According to Figure 5, it is implied the dates in Table 1 may not be the optimal boundaries of
 202 different phases, as there is no obvious share bike usage change after Feb 10.

203 We obtained a time series by computing the share bike usage within 200m of each POI every
 204 day in the period 02 Jan to 02 Mar 2020. The we segmented the time series into three phases using
 205 Definition 1 in Section 3.2. Here $k = 3$ and $N = 62$, we found the best classified phases with minimum
 206 sum of standard deviation using exhaustive search. According to the result in in Table 3, these phases
 207 can be identified as: before pandemics (a), during pandemics (b), pandemics mitigated (c).

Category	Split point 1	Split point 2
Tech company	23 Jan	24 Feb
Other company	23 Jan	28 Feb
RA	24 Jan	24 Feb
Subway station	24 Jan	24 Feb
Shopping plaza	24 Jan	24 Feb
Supermarket	24 Jan	24 Feb
Overall	23 Jan	24 Feb

Table 3. Segmentation of period 02 Jan to 02 Mar 2020

208 A minor difference between the share bike usage near companies and that near living facilities
 209 can be explained by a lag between the end of work and the start of vacation. Social and productive
 210 activities have not resumed until 24 Feb which is two weeks after the declaration of partial restart. The
 211 companies except for tech companies correspond mostly to real economy are delayed another one
 212 week.

213 We then computed the average share bike usage in these phases respectively.

Category	POI amount	Daily average bike usage within 200m radius of POIs per POI				
		a	b	c	b/a	c/a
Tech company	3858	200.4 ± 112.9	36.3 ± 14.4	41.1 ± 18.0	18.1%	20.5%
Other company	32301	162.5 ± 90.3	35.8 ± 14.5	39.4 ± 14.5	22.0%	24.2%
RA	5657	158.3 ± 86.9	36.6 ± 14.4	39.9 ± 13.9	23.1%	25.2%
Subway station	137	113.8 ± 66.6	29.0 ± 11.8	31.7 ± 10.6	25.5%	27.9%
Shopping plaza	217	168.9 ± 91.7	38.4 ± 14.6	41.0 ± 15.0	22.7%	24.3%
Supermarket	1076	137.6 ± 76.0	34.3 ± 13.4	37.7 ± 13.6	24.9%	27.4%

Table 4. Bike usage in different phases around the chosen POIs.

214 Table 4 depicts the bike usage of the six chosen categories. Ratio b/a shows that the bike usage
 215 of all categories decreased to one quarter, and tech companies dropped the most in both value and
 216 proportion, one possible explanation is they suit best “work from home”. Ratio c/a shows the bike
 217 usage of all categories has recovered to some extent but far from the situation of usual time after the
 218 partial restart of activities.

As can be inferred in Figure A2 and Figure A3 in Appendix, metro stations, and malls always position in the center of massive share bike clusters. In Figure A4, tech companies are crowded in the northwest of Beijing which takes the biggest share bike usage. However, mobility does not recover even after the pandemic was mitigated.

4.3. Co-location Analysis with Infected RAs

From Figure 3, we noticed that being the center of Beijing, Dongcheng and Xicheng district contain most of the infected RAs, and the confirmed time lies between 05 and 12 February. Like in Section 4.2, we adjusted the time intervals to match the confirmed time and carried the same analysis on the share bike usage around infected RAs and that of surrounding RAs (within the range of 1500m of infected RAs).

Category	RA amount	Daily average bike usage within 200m radius of RAs per RA				
		01 Jan-21 Jan (a)	05 Feb-12 Feb (b)	13 Feb-04 Mar (c)	b/a	c/a
Infected RA	19	160.8 ± 99.4	27.3 ± 22.7	43.2 ± 32.6	17.0%	26.9%
Surrounding RA	1591	139.2 ± 84.4	26.8 ± 20.1	38.7 ± 26.1	19.3%	27.8%
All RA	5657	158.3 ± 86.9	36.6 ± 14.4	39.9 ± 13.9	23.1%	25.2%

Table 5. Bike usage in different phases of infected RAs and that of surrounding RAs.

From Table 5, it can be inferred that the infected RAs suffered the most among the listed categories according to ratio b/a . Strict quarantine was practiced here to mitigate the pandemic. Surrounding RAs were also strongly impacted because of the residents got into a panic and keep themselves at home. According to ratio c/a , the share bike usage of infected RAs and their surrounding RAs have recovered roughly to the same level compared to other RAs from the pandemic.

As can be seen from the share bike usage of 16 Jan in Figure A1, the infected RAs are situated in the city center, with a huge pedestrian flow rate surrounded by massive share bikes. On 15 Feb, there is nearly no share bike usage around these infected RAs. On 2 Mar, nearly no massive share bike usage can be observed around the infected RAs, unlike metro stations and shopping plazas.

We can conclude the residents in Beijing followed exactly the suppression strategy whether the RAs were infected or not: quarantine, *cordon sanitaire*, and social distancing.

4.4. Spatiotemporal Patterns of Share Bike Usage

Figure 6 shows the spatial patterns of BSS activities from 21 Jan to 02 Mar by 4-day intervals, which is consistent with the changes detected in Figure 5. The daily share bike records are aggregated within 500-meter grids and rendered with a color ramp from grey to green to red (as is in Legend).

Before 21 Jan 2020, share bike activities were widely distributed throughout the city limits, with a significant concentration in the downtown area, which is orange or even red, corresponding to high-intensity activities (up to 500-1000 records/hour). These patterns could be regarded as a comprehensive reflection of the activities of the individuals in these regions and used as a reference to compare with that during the COVID-19 pandemic.

After the COVID-19 outbreak, there is a dramatic drop in mobility since 25 Jan, which was also the beginning of the Chinese New Year holidays. High-intensity activities could hardly be recognized in the subfigures between 25 Jan to 02 Feb. These subfigures are dominated by green and light green corresponding to low-intensity activities (<100 records/hour), indicating that individuals have demands to go out during this period, but unnecessary going-out has been significantly reduced by the combined effects of holidays and the epidemic. Status continued until 09 Feb, when the spread of COVID-19 was slowed down by imposing control measures including social distancing and home quarantine, and productive and social activities were allowed to restart partially.

Figure 6f-6k from 10 Feb to 01 Mar 2020, show a gradual increase in the mobility of the share bikes, but only restored around 30% of the pre-epidemic levels. As consistent with the Figure 5, there is a fluctuation near 14 Feb due to the increase in confirmed cases, which will be discussed in Section 5.2.

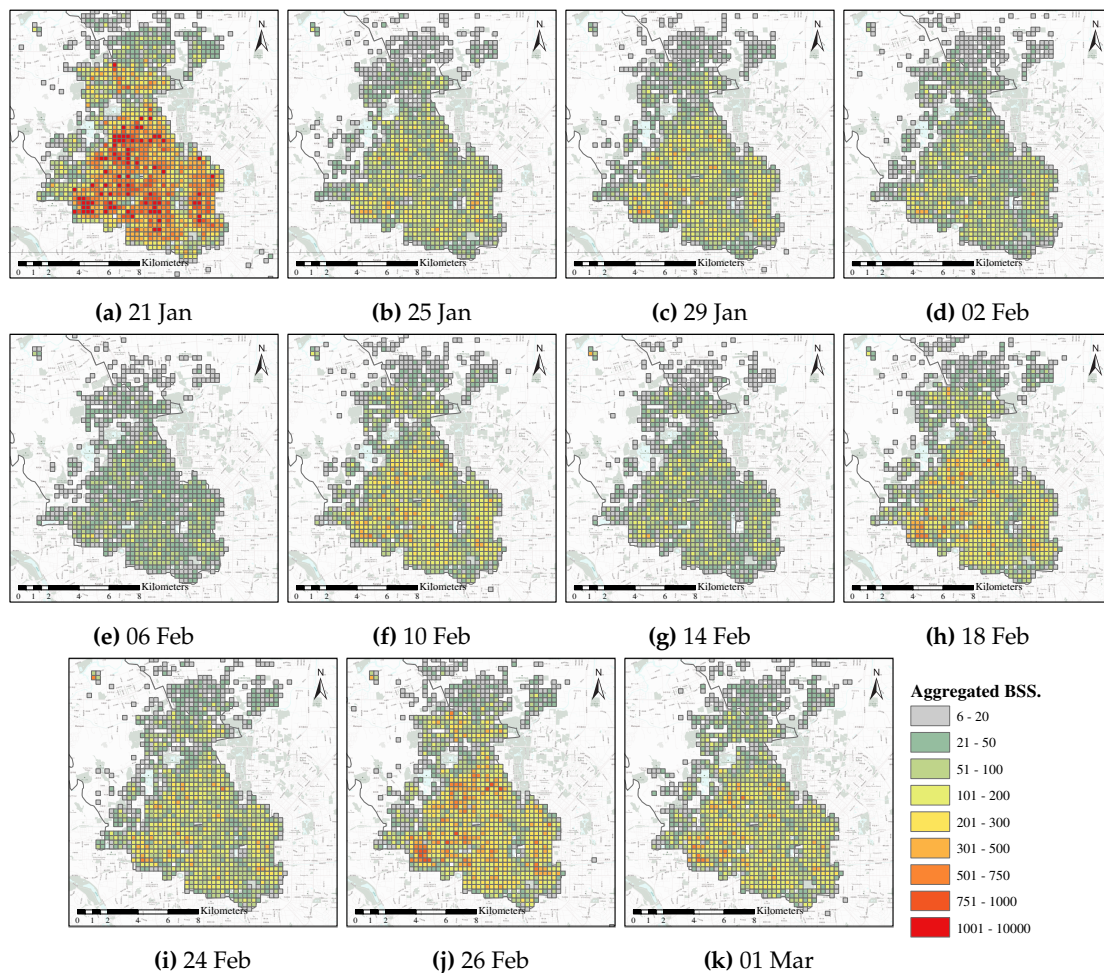


Figure 6. Spatial patterns of cycling activities from 21 Jan to 01 March 2020.

260 It is worth noticing that only slight differences could be observed between weekdays and weekends
 261 before 17 Feb and the weekday-weekend oscillation returned afterward.

262 There is a higher demand for share bikes on workdays in the downtown area than before.
 263 However, the high-intensity areas shrank on weekends, implying that residents were more inclined to
 264 reduce the risk of increased exposure by going outside under the threat of COVID-19.

265 The spatiotemporal analysis above verifies the segmentation of the outbreak timeline into 3 phases
 266 in Table 3:

- 267 • **Phase a:** dates before 21 Jan 2020, are considered as the first period when no strong
 268 COVID-19-specific interventions were imposed.
- 269 • **Phase b:** dates between 22 Jan and 17 Feb, include the Chinese New Year holiday 2020. During
 270 this period, traffic suspension and home quarantine were implemented for pandemics prevention
 271 purposes.
- 272 • **Phase c:** is after 17 Feb, when productive and social activities restarted partially since the
 273 pandemic was mitigated and under effective control.

274 5. Discussions

275 In this section, we first compare bike usage of 2019 and 2020, to demonstrate the influence of
 276 pandemic in residents activities apart from the impact of holiday. Associated with distribution of
 277 confirmed cases, the variations of behavior patterns are interpreted concerning different pandemic
 278 periods subsequently.

279 5.1. Comparison between 2019 and 2020

280 Both Chinese New Year holiday shutdowns and pandemic resulted in the aforementioned mobility
 281 decrease. Therefore, a comparison was conducted with data from the same period in 2019, thus
 282 removing the impact of the Chinese New Year holiday and evaluating the specific influence of the
 283 pandemic. The average values of aggregated daily share bike records from each pandemic phase were
 284 reported.

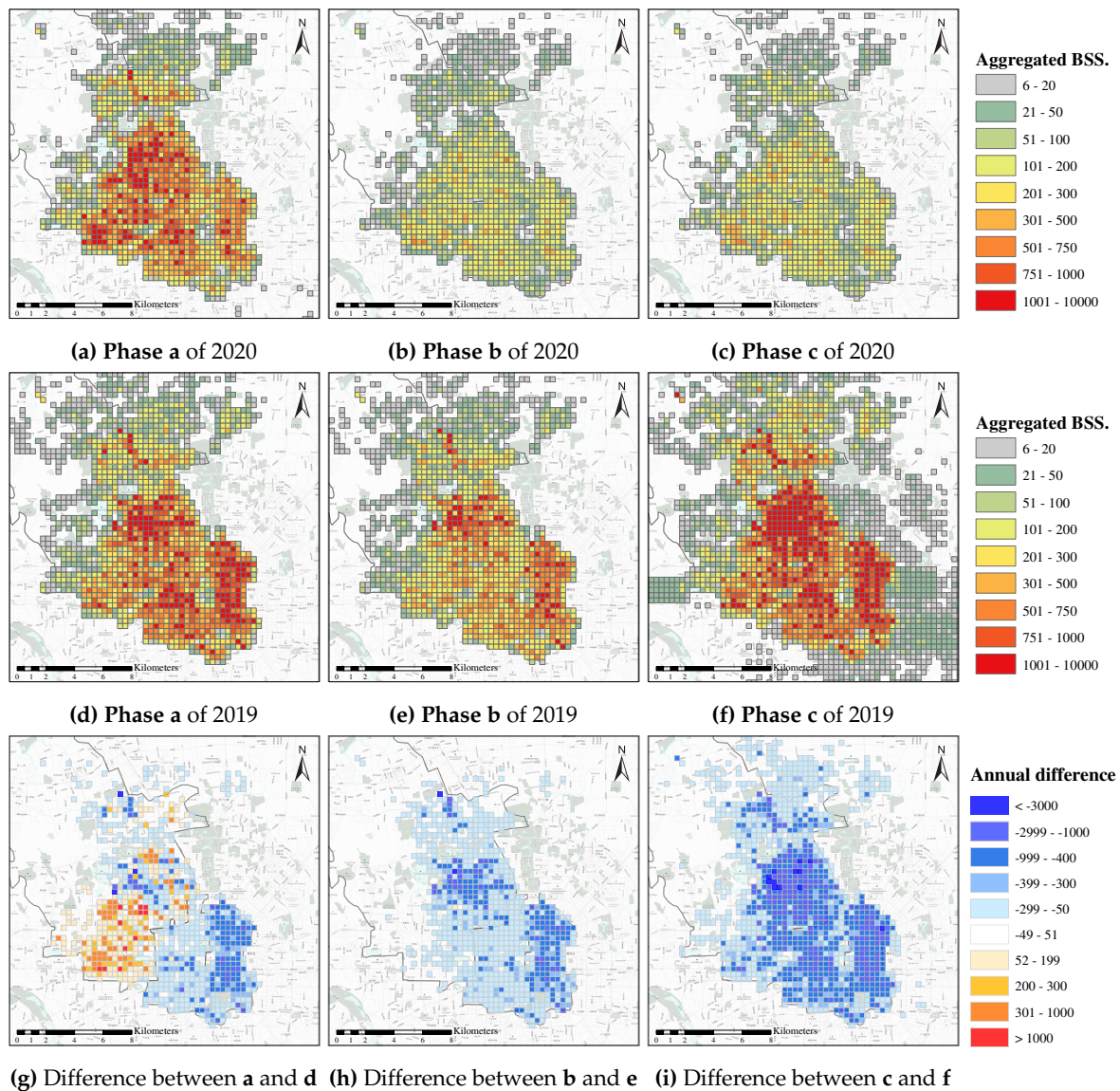


Figure 7. Comparison of share bikes usage between 2019 and 2020 in different pandemic periods.

285 Figure 7 delineates the results corresponding to 2020, 2019, and annual differences. Figure 7a-7c
 286 were consistent with the daily patterns during different pandemic stages presented in the previous
 287 section. Figure 7d summarized the averaged share bike intensity during the same time-interval as
 288 phase a in 2019, showing similar spatial patterns as 2020. Comparable numbers of positive and negative
 289 area could be observed from annual difference presented in Figure 7g. These discrepancies have
 290 relatively low values which could be attributed to the fluctuation of regional bike usage requirements.

291 The significant discrepancies in share bike usage between the year 2019 and 2020 during phase b
 292 and phase c is considered as the consequence of the pandemic of COVID-19. Normally, most migrants
 293 (34.6% of the population of Beijing) go back to their hometown during the Chinese New Year holiday;
 294 while permanent residents enjoy family gatherings and the main outdoor activity is visiting relatives

and friends. Therefore the holiday shutdowns reduced mobility in 2019, but high-intensity mobility could still be found in the urban districts from Figure 7e. Correspondingly, activities were in a state of complete suppression in 2020. The difference map in Figure 7h reveals the fact that under the impact of COVID-19, demands for outings were reduced for safety purposes.

In previous years, Figure 7f indicated that mobility would instantly return to pre-festival levels or more widespread as a result of the influx of migrant workers after the holiday. According to Figure 7c, the rehabilitation was in progress, but much slower during the epidemic mitigated period. The remarkable difference referred from Figure 7i verified this sustained impact on the daily lives of citizens.

5.2. Relationships between Share Bike Usage and Confirmed Cases during Pandemic Periods

This part aims at characterizing the variations of behavior patterns by evaluating share bike usage concerning different pandemic periods. Figure 8 shows the share bike usage in **phase b**, i.e., the quarantine period. Same as previous sections, aggregated share bike records were rendered with a color ramp from grey to green to red. Confirmed cases in each district are displayed by blue circles, where the cumulative number of cases is shown by the size of circles. When comparing the panels from left to right with the date varying from 25 Jan to 08 Feb, we observe that the aggregated share bike intensity gradually decreases with an increasing number of confirmed cases and then remains at a low level. The aggregated share bike intensity in the downtown area changed from red to green. Starting on January 25, 2020, highly restrictive measures were implemented by local government: individuals were asked to follow a series of social distancing measures. As a result, the number of newly confirmed COVID-19 cases was effectively suppressed.

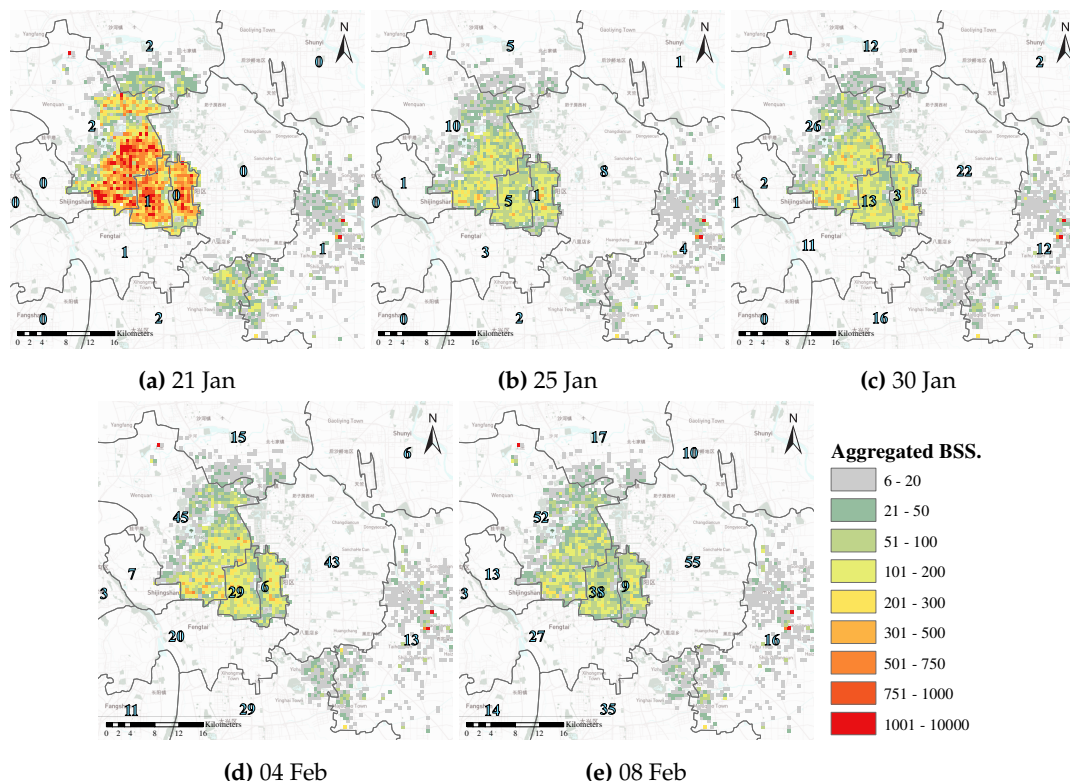


Figure 8. Relationships between aggregated share bike records and confirmed cases during **phase b**.

Figure 9 depicts the share bike usage in **phase c**, when productive and social activities were allowed to restart partially.

During the mitigation period, aggregated share bike usage gradually rebounded with stable accumulated confirmed cases during the weekdays, which can be inferred from Figure 11a–Figure 11e.

320 The recovery of the city is unbalanced in the spatial domain, concentrating in urban districts, whereas
 321 changes are not significant in other areas. Another finding is the different patterns between weekdays
 322 and weekends. A reduction in mobility on weekends could be inferred from the comparison between
 323 Figure 11e and Figure 11f, which was attributed to the awareness of the risk of infection of residents.

324 It should be highlighted that the accumulated confirmed cases stay substantially stable across this
 325 period, suggesting control measures were effective and necessary in the containment of the spread of
 326 COVID-19 during the resilience of Beijing.

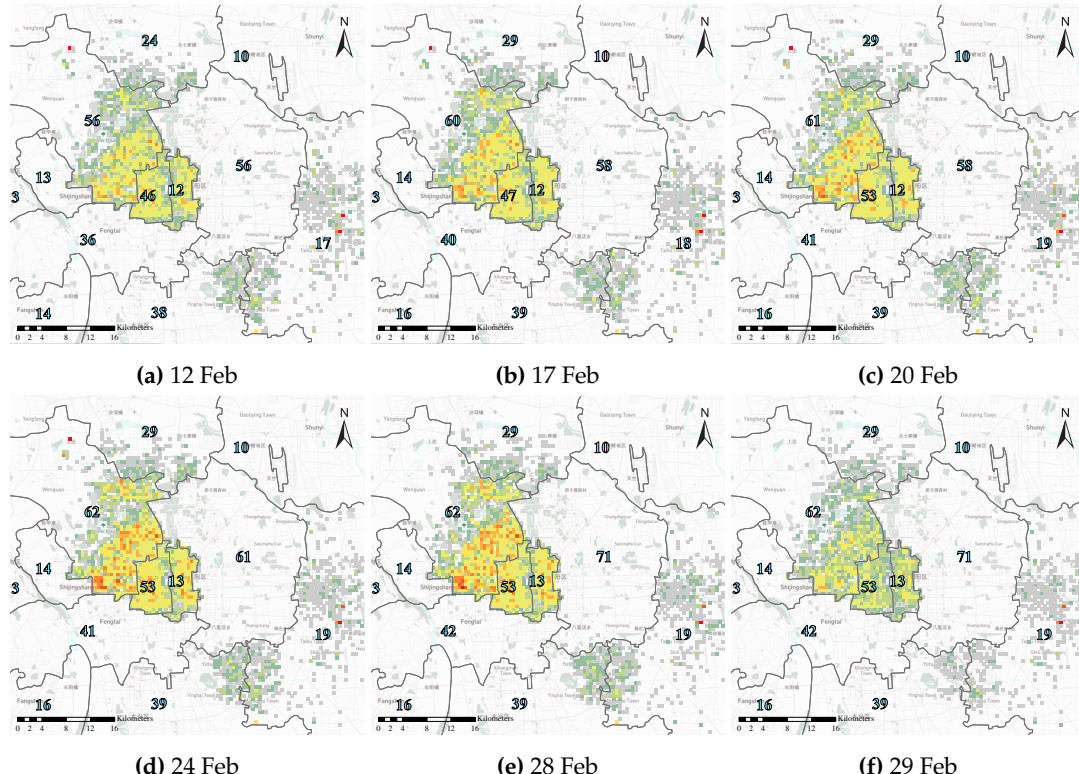


Figure 9. Relationships between aggregated share bike records and confirmed cases during phase c.

327 6. Conclusion

328 The wide-spread BSS is an alternative data source for characterizing the spatial and temporal
 329 detail of the mobility and the activities of residents. Motivated by the current COVID-19 outbreak and
 330 rapid development in BSS, this paper constructs a framework targeting at extracting and analyzing
 331 behavior pattern based on long time-sequenced share bike usage.

332 Based on share bike usage, we investigated the impact of the pandemic on the behavior of
 333 residents and the rehabilitation process on the city scale. After removing the factor of the Chinese New
 334 Year holiday, our results suggest that social and productive activities of residents were hugely affected
 335 by the COVID-19, reflected in the drastic decrease of share bike usage (down to less than 40% of that
 336 of the same period in 2019). It can be figured out that the cumulative confirmed cases stayed stable
 337 substantially after the restarting of productive activities, implying the ongoing control measures were
 338 necessary and effective in the containment of the spread of COVID-19 when opening-up. Co-location
 339 analysis shows the infected RAs situated in the city center are most impacted, even after the pandemic
 340 is mitigated; Among POIs, share bike usage of tech companies has the biggest change before and
 341 during the pandemic as these companies are most suitable for “work from home”, etc. These findings
 342 provide supplementary details to the public reactions during the pandemic. As the situation develops
 343 globally, our results could be references to epidemiological researches and inform policymaking in the

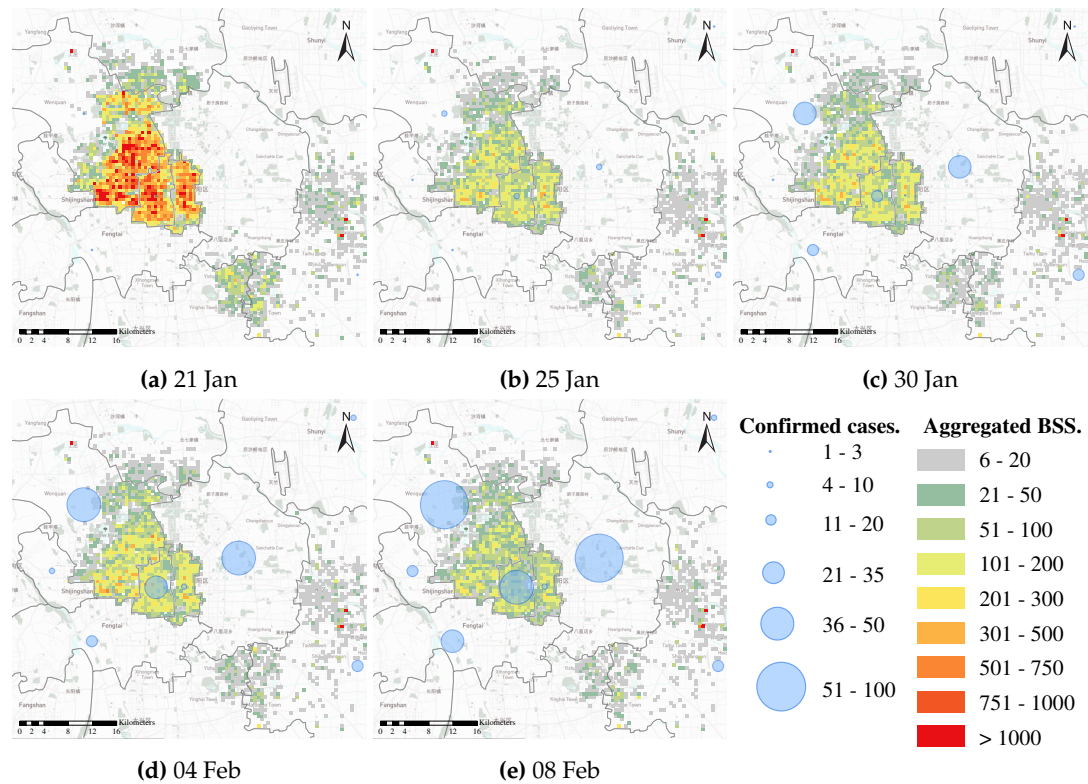


Figure 10. Relationships between aggregated share bike records and confirmed cases during phase b.

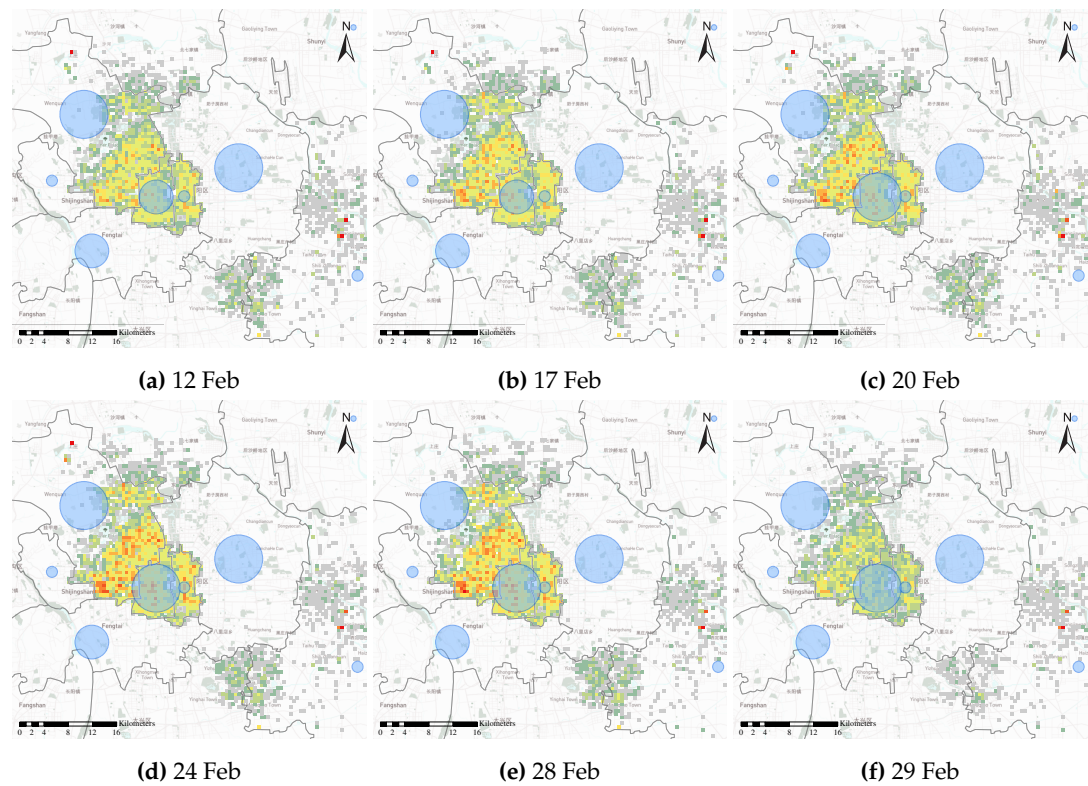


Figure 11. Relationships between aggregated share bike records and confirmed cases during phase c.

344 context of the current COVID-19 outbreak, and help to prevent the emergence of pandemics in the
 345 future.

346 7. Future Work

347 Since the government implemented multiple interventions at the same time or in a short timeframe
 348 to control the outbreak, individual strategies could not be evaluated. Multi-dimensional principal
 349 component analysis could be helpful to extract the modes contributed by each preventive measure.

350 Also, our current work has extracted the features of mobility reflected by BSS. Another possible
 351 extension is to build a dynamic model based on the features predicting the share bike usage and
 352 potential social event/reaction of the public during the pandemic or emergencies.

353 **Acknowledgments:** This study was supported by the National Key R&D Program of China (2017YFB0503700
 354 and 2018YFB2100701), the Research Program of Beijing Advanced Innovation Center for Future Urban Design
 355 (UDC2019031321), and the National Natural Science Foundation of China (41601389).

356 Abbreviations

357 The following abbreviations are used in this manuscript:

BSS Bike Sharing System

GIS Geographic Information System

358 POI Point Of Interest

RA Residential Area

VGI Volunteered Geographical Information

359 Appendix A Figures Illustrating Colocation Patterns with POIs

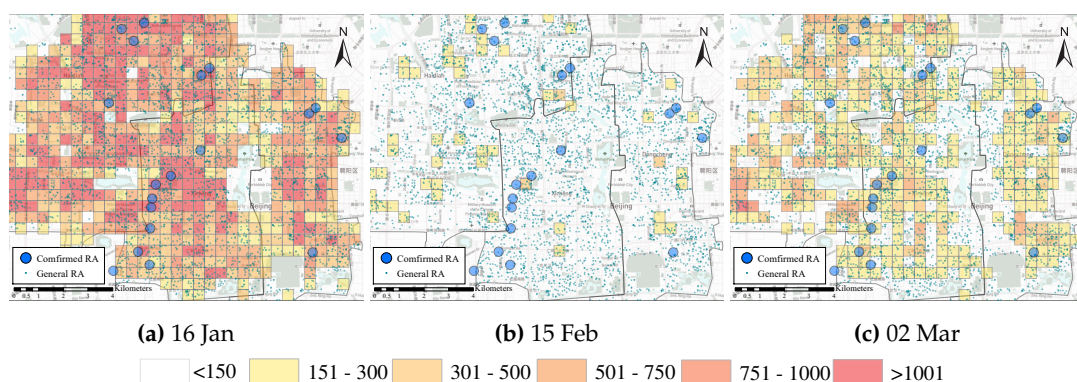


Figure A1. Share bikes and RAs.

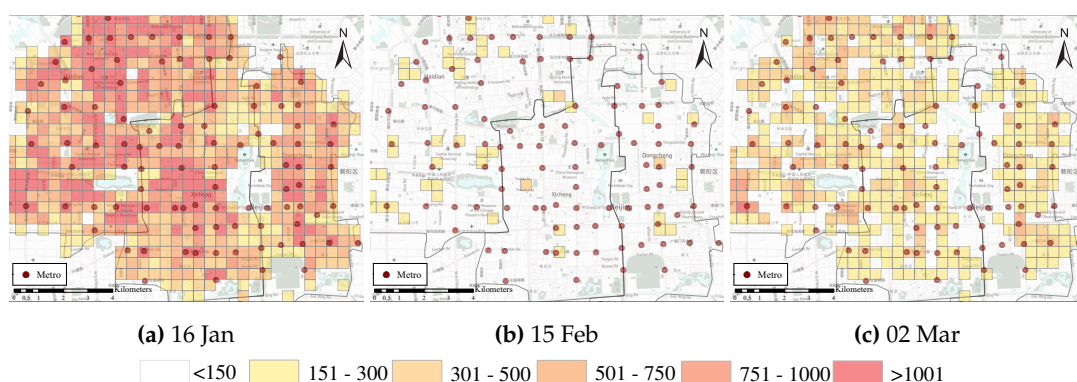


Figure A2. Share bikes and metro stations.

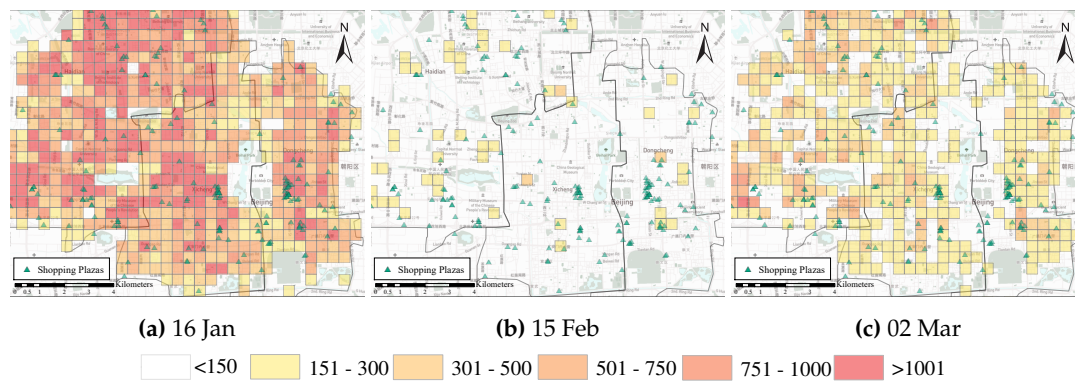


Figure A3. Share bikes and shopping plazas.

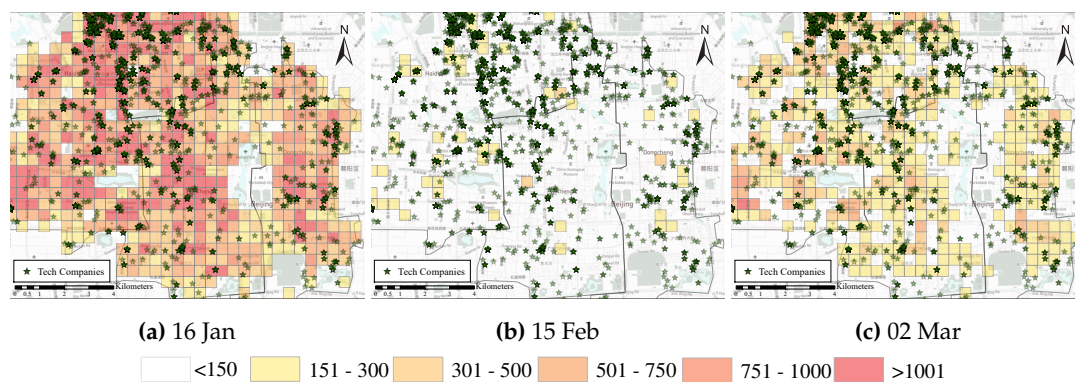


Figure A4. Share bikes and tech companies.

360 References

- 361 1. Wang, Y.; Chen, C.; Wang, J.; Baldick, R. Research on Resilience of Power Systems Under Natural
362 Disasters—A Review. *IEEE Transactions on Power Systems* **2016**, *31*, 1604–1613.

363 2. Akter, S.; Wamba, S.F. Big data and disaster management: a systematic review and agenda for future
364 research. *Annals of Operations Research* **2019**, *283*, 939–959.

365 3. Li, Q.; Guan, X.; Wu, P.; Wang, X.; Zhou, L.; Tong, Y.; Ren, R.; Leung, K.S.; Lau, E.H.; Wong, J.Y.; others.
366 Early transmission dynamics in Wuhan, China, of novel coronavirus–infected pneumonia. *New England
367 Journal of Medicine* **2020**.

368 4. Pitzer, V.E.; Viboud, C.; Simonsen, L.; Steiner, C.; Panizzo, C.A.; Alonso, W.J.; Miller, M.A.; Glass, R.I.;
369 Glasser, J.W.; Parashar, U.D.; others. Demographic variability, vaccination, and the spatiotemporal
370 dynamics of rotavirus epidemics. *Science* **2009**, *325*, 290–294.

371 5. Chinazzi, M.; Davis, J.T.; Ajelli, M.; Gioannini, C.; Litvinova, M.; Merler, S.; y Piontti, A.P.; Rossi, L.; Sun, K.;
372 Viboud, C.; others. The effect of travel restrictions on the spread of the 2019 novel coronavirus (2019-nCoV)
373 outbreak. *medRxiv* **2020**.

374 6. Van den Hazel, P.; Zuurbier, M.; Babisch, W.; Bartonova, A.; Bistrup, M.L.; Bolte, G.; Busby, C.; Butter,
375 M.; Ceccatelli, S.; Fucic, A.; others. Today’s epidemics in children: possible relations to environmental
376 pollution and suggested preventive measures. *Acta Paediatrica* **2006**, *95*, 18–25.

377 7. Ferguson, N.; Laydon, D.; Nedjati Gilani, G.; Imai, N.; Ainslie, K.; Baguelin, M.; Bhatia, S.; Boonyasiri,
378 A.; Cucunuba Perez, Z.; Cuomo-Dannenburg, G.; others. Report 9: Impact of non-pharmaceutical
379 interventions (NPIs) to reduce COVID19 mortality and healthcare demand. Technical report, Imperial
380 College London, 2020.

381 8. Song, C.; Koren, T.; Wang, P.; Barabási, A.L. Modelling the scaling properties of human mobility. *Nature
382 Physics* **2010**, *6*, 818–823.

383 9. Song, X.; Zhang, Q.; Sekimoto, Y.; Shibasaki, R. Prediction of Human Emergency Behavior and Their
384 Mobility Following Large-Scale Disaster. Proceedings of the 20th ACM SIGKDD International Conference
385 on Knowledge Discovery and Data Mining, 2014, p. 5–14.

- 386 10. Yu, M.; Yang, C.; Li, Y. Big Data in Natural Disaster Management: A Review. *Geosciences* **2018**, *8*, 165.
- 387 11. Goodchild, M.F.; Glennon, J.A. Crowdsourcing geographic information for disaster response: a research
388 frontier. *International Journal of Digital Earth* **2010**, *3*, 231–241.
- 389 12. Huang, W.; Li, S.; Liu, X.; Ban, Y. Predicting human mobility with activity changes. *International Journal of
390 Geographical Information Science* **2015**, *29*, 1569–1587.
- 391 13. Horanont, T.; Witayangkurn, A.; Sekimoto, Y.; Shibasaki, R. Large-Scale Auto-GPS Analysis for Discerning
392 Behavior Change during Crisis. *IEEE Intelligent Systems* **2013**, *28*, 26–34.
- 393 14. Wilson, R.; Zu Erbach-Schoenberg, E.; Albert, M.; Power, D.; Tudge, S.; Gonzalez, M.; Guthrie, S.;
394 Chamberlain, H.; Brooks, C.; Hughes, C.; Pitonakova, L.; Buckee, C.; Lu, X.; Wetter, E.; Tatem, A.;
395 Bengtsson, L. Rapid and Near Real-Time Assessments of Population Displacement Using Mobile Phone
396 Data Following Disasters: The 2015 Nepal Earthquake. *PLoS currents* **2016**, *8*, 267–270.
- 397 15. Chae, J.; Thom, D.; Jang, Y.; Kim, S.; Ertl, T.; Ebert, D.S. Public behavior response analysis in disaster events
398 utilizing visual analytics of microblog data. *Computers & Graphics* **2014**, *38*, 51–60.
- 399 16. Wesolowski, A.; Eagle, N.; Tatem, A.J.; Smith, D.L.; Noor, A.M.; Snow, R.W.; Buckee, C.O. Quantifying the
400 Impact of Human Mobility on Malaria. *Science* **2012**, *338*, 267–270.
- 401 17. Li, S.; Dragicevic, S.; Castro, F.A.; Sester, M.; Winter, S.; Coltekin, A.; Pettit, C.; Jiang, B.; Haworth, J.; Stein,
402 A.; Cheng, T. Geospatial big data handling theory and methods: A review and research challenges. *ISPRS
403 Journal of Photogrammetry and Remote Sensing* **2016**, *115*, 119–133.
- 404 18. Mobike and Ofo: Reinventing the Bike-Sharing Business Model in China. [https://daxueconsulting.com/
405 mobike-and-ofo-bike-sharing/](https://daxueconsulting.com/mobike-and-ofo-bike-sharing/).
- 406 19. Du, M.; Cheng, L. Better understanding the characteristics and influential factors of different travel patterns
407 in free-floating bike sharing: Evidence from Nanjing, China. *Sustainability* **2018**, *10*, 1244.
- 408 20. Xu, Y.; Chen, D.; Zhang, X.; Tu, W.; Chen, Y.; Shen, Y.; Ratti, C. Unravel the landscape and pulses of
409 cycling activities from a dockless bike-sharing system. *Computers, Environment and Urban Systems* **2019**,
410 *75*, 184–203.
- 411 21. Pal, A.; Zhang, Y. Free-floating bike sharing: Solving real-life large-scale static rebalancing problems.
412 *Transportation Research Part C: Emerging Technologies* **2017**, *80*, 92–116.
- 413 22. Ai, Y.; Li, Z.; Gan, M.; Zhang, Y.; Yu, D.; Chen, W.; Ju, Y. A deep learning approach on short-term
414 spatiotemporal distribution forecasting of dockless bike-sharing system. *Neural Computing and Applications*
415 **2019**, *31*, 1665–1677.
- 416 23. Chen, L.; Zhang, D.; Wang, L.; Yang, D.; Ma, X.; Li, S.; Wu, Z.; Pan, G.; Nguyen, T.M.T.; Jakubowicz, J.
417 Dynamic cluster-based over-demand prediction in bike sharing systems. Proceedings of the 2016 ACM
418 International Joint Conference on Pervasive and Ubiquitous Computing, 2016, pp. 841–852.
- 419 24. Huang, Z.; Chen, Y.; Wan, L.; Peng, X. GeoSpark SQL: An effective framework enabling spatial queries on
420 Spark. *ISPRS International Journal of Geo-Information* **2017**, *6*, 285.
- 421 25. Terzi, E.; Tsaparas, P. Efficient algorithms for sequence segmentation. Proceedings of the 2006 SIAM
422 International Conference on Data Mining. SIAM, 2006, pp. 316–327.

423 © 2020 by the authors. Submitted to *ISPRS Int. J. Geo-Inf.* for possible open access
424 publication under the terms and conditions of the Creative Commons Attribution (CC BY) license
425 (<http://creativecommons.org/licenses/by/4.0/>).